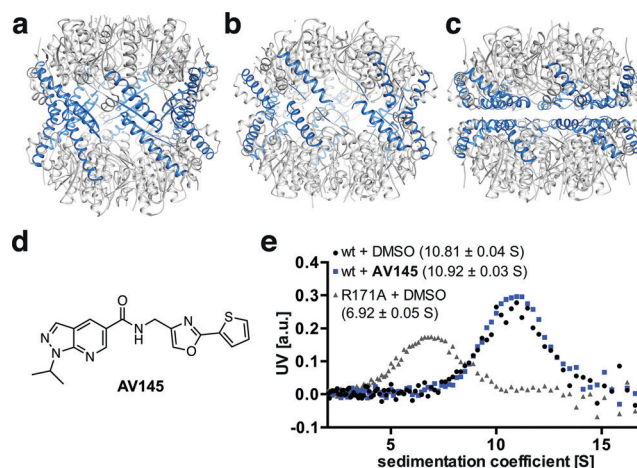**Drug Development**

Reversible Inhibitors Arrest ClpP in a Defined Conformational State that Can Be Revoked by ClpX Association

Axel Pahl, Markus Lakemeyer, Marie-Theres Vielberg, Mathias W. Hackl, Jan Vomacka, Vadim S. Korotkov, Martin L. Stein, Christian Fetzer, Katrin Lorenz-Baath, Klaus Richter, Herbert Waldmann, Michael Groll,* and Stephan A. Sieber*

Abstract: *Caseinolytic protease P (ClpP) is an important regulator of Staphylococcus aureus pathogenesis. A high-throughput screening for inhibitors of ClpP peptidase activity led to the identification of the first non-covalent binder for this enzyme class. Co-crystallization of the small molecule with S. aureus ClpP revealed a novel binding mode: Because of the rotation of the conserved residue proline 125, ClpP is locked in a defined conformational state, which results in distortion of the catalytic triad and inhibition of the peptidase activity. Based on these structural insights, the molecule was optimized by rational design and virtual screening, resulting in derivatives exceeding the potency of previous ClpP inhibitors. Strikingly, the conformational lock is overturned by binding of ClpX, an associated chaperone that enables proteolysis by substrate unfolding in the ClpXP complex. Thus, regulation of inhibitor binding by associated chaperones is an unexpected mechanism important for ClpP drug development.*

Figure 1. SaClpP in its a) extended (PDB ID: 3V5E), b) compact (PDB ID: 4EMM), and c) compressed (PDB ID: 3QWD) state. The E helices are shown in blue. d) Structure of **AV145**. e) Analytical ultracentrifugation of wild-type ClpP and the heptameric[2] ClpP mutant R171A. DMSO served as a control. Sedimentation coefficient maxima are shown as the mean ± standard deviation.

Caseinolytic protease P (ClpP), a member of the serine hydrolase enzyme family, is a major regulator of bacterial cell homeostasis.[1] The enzymatic complex consists of two adjacent heptameric rings that are connected by central α-helices E, forming a tetradecameric barrel (Figure 1 a–c). The E helix is linked to strand β9, which forms crucial hydrogen bonds across the heptamer interface. Different conformations of ClpP have been observed. Whereas an extended E helix (Figure 1 a, PDB ID: 3V5E)[2] is important for peptidolytic activity and tetradecamer stability, a kink in this helix leads to either compact (Figure 1 b, PDB ID: 4EMM)[3] or compressed (Figure 1 c, PDB ID: 3QWD)[4] states with misaligned catalytic triads. This distortion of catalytic residues induces a rotation of the conserved Pro125 (in strand β9), which in turn pulls at helix E, resulting in its collapse. ClpP requires associated chaperones, such as hexameric ClpX, to unfold and digest larger protein substrates.[1] Moreover, ClpX binding is believed to induce conformational selection of the active and extended state.[5]

Thus far, only β-lactones and phenyl esters have been reported as specific ClpP inhibitors in whole proteome studies.[6] Both compound classes covalently acylate the active-site Ser98.[7] Covalent, irreversible binding is beneficial for proteome-labeling experiments, mechanistic studies, and for achieving a prolonged target residence time. The in vitro[5,6] and in vivo[8] application of irreversible ClpP inhibitors, however, has been limited by the low stability of their electrophilic motifs owing to hydrolysis.[9] Thus far, all attempts to design non-covalent inhibitors have failed.[7a] Surprisingly, given the importance of ClpP inactivation and the need for rational design, only one complex crystal structure of the protease with a nonspecific chloromethyl ketone (CMK) peptide ligand is available (PDB ID: 2FZS).[10] Herein, we report the first co-crystal structure of a specific ClpP inhibitor with a novel, reversible mode of action, which was further exploited to synthetically optimize the ligand by rational design and in silico screening.

[*] Dr. A. Pahl,[+] M. Lakemeyer,[+] M.-T. Vielberg,[+] M. W. Hackl, J. Vomacka, Dr. V. S. Korotkov, Dr. M. L. Stein, C. Fetzer, Dr. K. Lorenz-Baath, Dr. K. Richter, Prof. Dr. M. Groll, Prof. Dr. S. A. Sieber
Center for Integrated Protein Science at the Department of Chemistry, Technische Universität München
Lichtenbergstrasse 4, 85747 Garching (Germany)
E-mail: michael.groll@tum.de
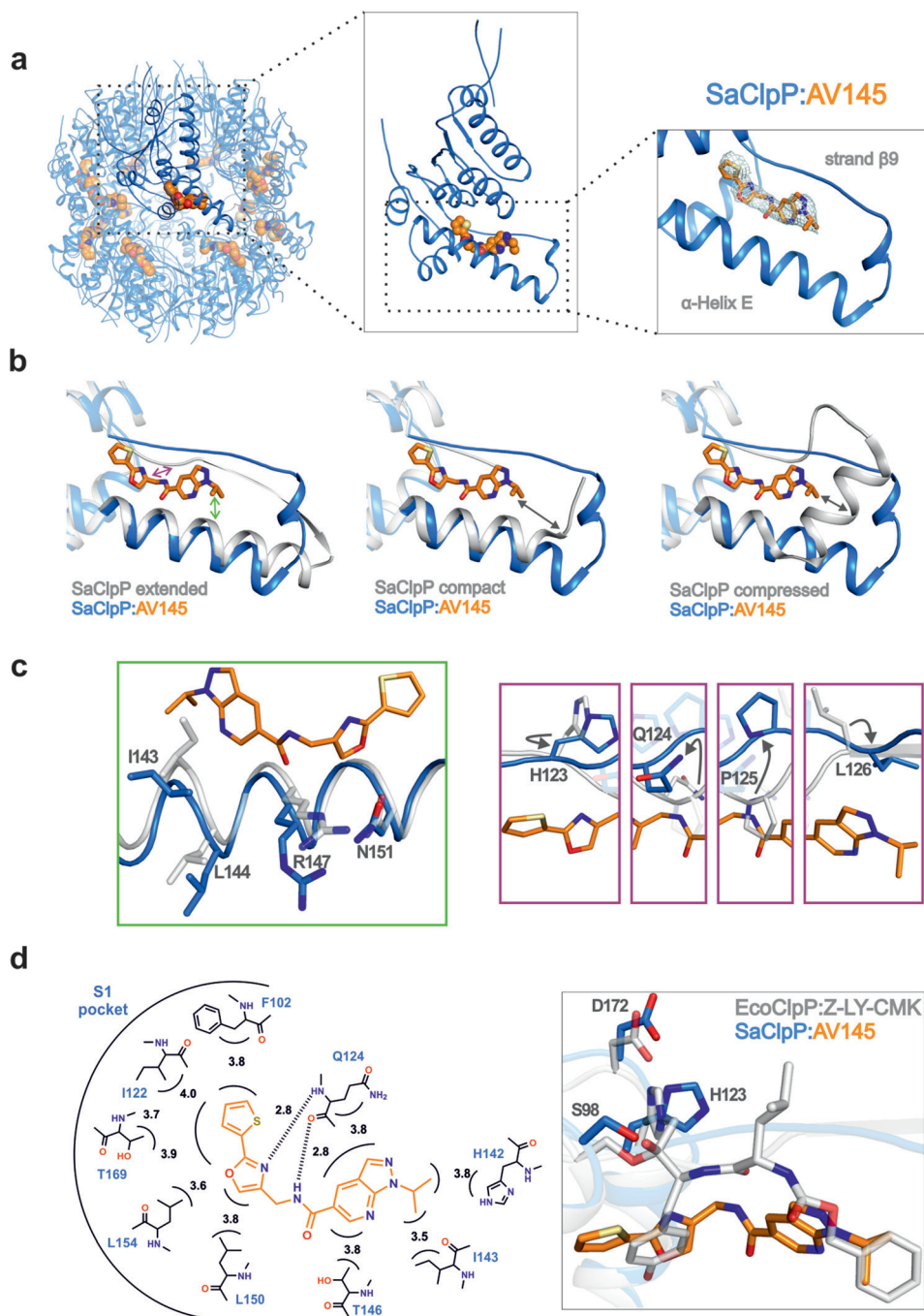stephan.sieber@tum.de

Prof. Dr. H. Waldmann
Department of Chemistry and Chemical Biology
Technische Universität Dortmund
Otto-Hahn-Strasse 6, 44221 Dortmund (Germany)

[+] These authors contributed equally to this work.

Supporting information and ORCID(s) from the author(s) for this article are available on the WWW under http://dx.doi.org/10.1002/anie.201507266.

A previous high-through-put screen (HTS) with about 140000 compounds from the COMAS library (MPI Dort-mund) did not reveal a single non-covalently binding SaClpP inhibitor with an $IC_{50} < 2$ μm.[6a] However, the low activity of ClpP with the standard Suc-Leu-Tyr-AMC substrate requires at least 1 μm ClpP to record significant turnover, so that the potencies of the best inhibitors are still in the micro-molar concentration range. We therefore reinvestigated our previous HTS results by low-ering the selection criteria to an $IC_{50} \le 10$ μm.[6a] Four com-pounds of the HTS fulfilled this prerequisite (Supporting Information, Figure S1). Mass-spectrometric analysis of the intact proteins revealed that **AV145** binds non-covalently (Figure 1d, Figure S1), and medicinal-chemistry considera-tions made this compound the most promising candidate for further analysis. Compound **AV145** lacks any reactive groups and consists of three characteristic heterocycles, a pyrazolopyridine as well as a 2-(thiophen-2-yl)oxazole moiety. Time-dependent incu-bation of SaClpP with **AV145** did not change the IC_{50} (Fig-ure S2), supporting the fact that the compound is a reversi-ble inhibitor. Furthermore, analytical ultracentrifugation demonstrated that **AV145**, unlike most phenyl esters and lactones, did not induce disso-ciation of ClpP into heptamers (Figure 1e).[6a, 7b]

To gain insights into the mechanism of inhibition, we co-crystallized **AV145** with SaClpP and solved the complex structure by molecular replace-ment at 3 Å resolution ($R_{\text{free}} =$
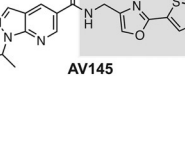

Figure 2. a) Binding of **AV145** to SaClpP (PDB ID: 5DL1). b) Structural superposition of SaClpP:**AV145** with the extended, compact, or compressed form of SaClpP. Structural changes between the extended and co-crystal structure are indicated by colored arrows. c) Detailed exploration of the structural changes of α-helix E and strand β9 compared to the extended form. d) Analysis of the specific enzyme–inhibitor contacts and overlay with the EcoClpP:Z-LY-CMK structure (PDB ID: 2FZS), illustrating the non-covalent inhibition mechanism of **AV145**. Color code: SaClpP:AV145 marine, AV145 orange, SaClpP:extended/compact/compressed and EcoClpP:Z-LY-CMK gray; heteroatoms: O red, N blue, S yellow.

27.4%, Table S1, PDB ID: 5DL1). The asymmetric unit contains a ClpP tetradecamer with the compound bound to every subunit. Despite variations in occupancy, model build-ing into the averaged $2F_o-F_c$ electron-density map allowed the unambiguous positioning of **AV145** near to the active site between α-helix E and strand β9 (Figure 2a). Surprisingly,

overlays with structures of the apo enzyme in its extended, compact, and compressed form revealed that the inhibitor binds in a non-substrate-like mode and induces an unprece-dented conformational state (Figure 2b). Although helix E is almost completely aligned as in the extended, active enzyme, binding of **AV145** displaces Ile143 and Arg147 because of

a steric clash (Figure 2c) leading to a shift of about 1.4 Å in the center of the helix (green arrow in Figure 2b). The majority of the structural alterations, however, are found in strand β9 (purple arrow in Figure 2b). Formation of a β-sheet with the subunit in the opposite ring is impeded, as can be seen by the partial disorder of the two glycine residues 127 and 128. Notably, β9 is mainly defined by a large inhibitor-induced flip of Pro125 of about 180°. The residue still retains its *trans* peptide bond and resides at a similar position as in the inactive form of the protease (Figure 2c). One direct consequence of this relocation is a shift of His123 out of the catalytic triad, leading to a distortion of the active site, which explains the inhibiting effect of **AV145**. The induced structural rearrangement of Pro125 also causes a major change to Gln124. Hereby, Gln124 is arrested in a position where it is able to form two hydrogen bonds between its peptide backbone and **AV145**, likely providing important protein–inhibitor interactions. Moreover, an extended network of van

der Waals contacts with Phe102, Ile122, His142, Ile143, Thr146, Leu150, and Leu154 as well as Thr169 stabilizes compound binding (Figure 2d). Overall, this novel mode of action explains why **AV145** is a non-covalent SaClpP inhibitor. Superposition of our structure with the Z-LY-CMK bound EcClpP structure (PDB ID: 2FZS)[10] reveals differences (Figure 2d). Unlike CMK, **AV145** does not influence the catalytic center of SaClpP directly, but rather transmits its function through neighboring residues. Such a type of indirect binding has not been observed for this class of enzymes thus far.

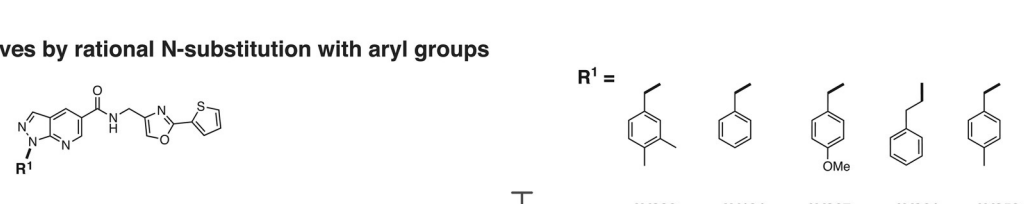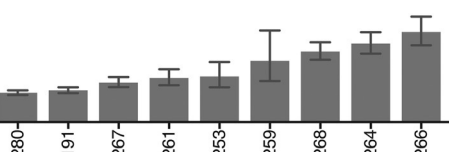The co-crystal structure of SaClpP in complex with **AV145** provides key information for improving inhibitor potency. The two constituent parts of the molecule, namely the pyrazolopyridine (acid part) and 2-(thiophen-2-yl)oxazole (amine part) moieties, were substituted with different chemical groups to explore their structure–activity relationships (SARs; Figure 3a). Compounds were designed according to

Figure 3. SAR studies. a) The amine part of **AV145** is intolerant to modifications whereas the acid part can be modified to improve ClpP inhibition. b) Synthesis of **AV280**: Reagents and conditions: i) 3,4-dimethylbenzyl bromide, K$_2$CO$_3$, DMF, RT, 18 h; ii) LiOH, THF/H$_2$O (9:1), RT, 18 h; iii) neat, 120 °C, 16 h; iv) NaN$_3$, DMF, 60 °C, 16 h; v) PPh$_3$, THF/H$_2$O (9:1), RT, 16 h; vi) TBTU, NMM, DMF, 0 °C to RT, 18 h. Structures and IC$_{50}$ values for derivatives with c) *N*-aryl substituents and d) *para*-substituted aryl groups that were inspired by virtual screening. IC$_{50}$ values are derived from at least two biological experiments with three technical replicates per concentration and are shown as mean and 95% confidence interval. See the Supporting Information for further details.
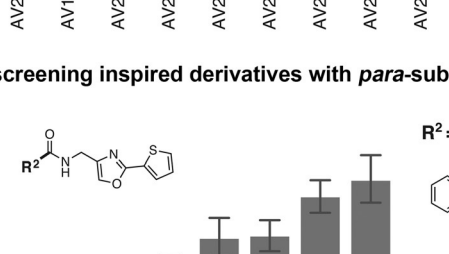
rational considerations or resulted from a virtual screen (see the Supporting Information). Alterations within the amine part, for example, by introduction of thiophene substituents and the replacement of the thiophene by a phenyl or oxazole group, resulted in inactive compounds (Figures S3, S4). However, modifications within the acid part were much more tolerated and led to improved inhibitors. Based on this, we explored the possibility of incorporating aromatic groups for π-stacking with His142 (part of the strand β9) through the design of eleven derivatives with *N*-aryl substituents (Figure 3 c).

The synthesis of these derivatives, exemplified for **AV280** in Figure 3 b, involved N-alkylation of pyrazolopyridine **1** with 3,4-dimethylbenzyl bromide, followed by saponification of the ester with lithium hydroxide. Preparation of the oxazole amine part **3** started with the condensation of the appropriate aryl amide with dichloroacetone at 120°C. The resulting chloromethyl-substituted oxazole **2** was converted into amine **3** in two steps. Standard amide coupling of the acid with the amine resulted in the final products.

AV191 and **AV280**, which bear a benzyl and a 3,4-dimethylbenzyl substituent, respectively, showed a sixfold increase in ClpP inhibition compared to **AV145**, with IC_{50} values of 1.7 and 1.5 μM, respectively (Figure 3 c). Based on results from the virtual screening, we next replaced the pyrazolopyridine moiety by aryl rings with a *para* urea or a *para* carbamate substituent, resulting in **AV286** with an IC_{50} value of 0.9 μM (Figure 3 d). Notably, this value shows that a stoichiometric amount of **AV286** (relative to the monomer concentration of the protease) is sufficient to inhibit 50% of SaClpP. An increase in substrate concentration did not influence inhibitor binding (Figure S5).

With potent and reversible ClpP inhibitors at hand, we investigated whether the best compound of this series exhibits cell permeability and target selectivity in situ. Therefore, an **AV286**-related activity-based protein profiling[11] photoprobe (**AV321**) equipped with a diazirine photocrosslinker and an alkyne tag was prepared (Figure 4 a).[12] Pleasingly, the probe retained a low IC_{50} value (2 μM) for SaClpP peptidase inhibition (Figure S6). Living *S. aureus* cells were incubated with **AV321**, irradiated with UV light to form a covalent link between target protein and diazirine, lysed, and clicked to a functionalized azide tag (fluorescent dye or biotin) via the alkyne; the labeled proteome was then analyzed by fluorescence SDS-PAGE analysis (Figure 4 b) or mass spectrometry (MS; Figure 4 c). A dominant fluorescent protein band at the molecular weight of ClpP appeared on SDS-PAGE (Figure 4 b). To confirm ClpP binding in situ we performed quantitative gel-free MS by isotope labeling.[13] MS-based target enrichment was visualized by volcano plots (Figure 4 c, Figure S7). In all runs, ClpP was highly enriched, and only a few putative off-targets (significance level: $p \leq 0.05$), such as the 50S ribosomal protein L1 (Protein ID ID: Q2G0P0), were detected. We next examined whether cell-permeable inhibitors reduced the production of α-hemolysin (hla), a predominant *S. aureus* toxin regulated by ClpP. Surprisingly, the general level of hla was high, suggesting that inhibition of intracellular proteolysis was not as efficient as the reduction of in vitro peptidase activity.
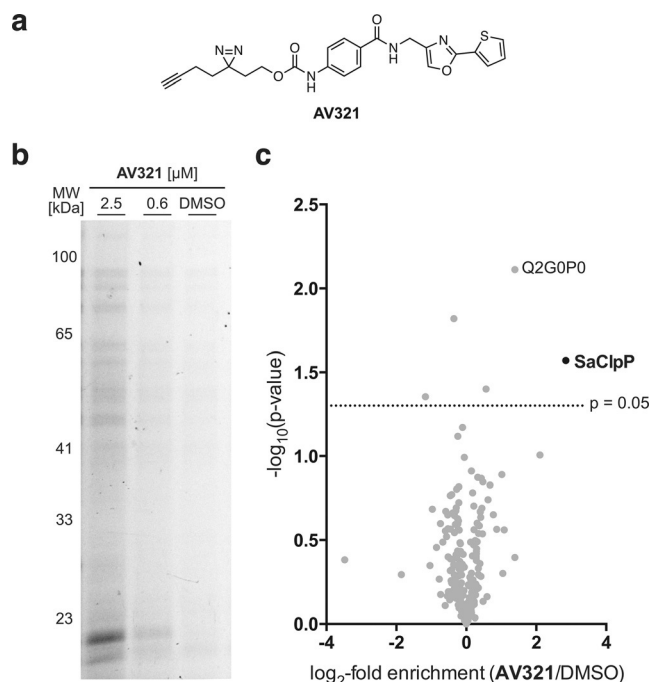
Figure 4. In situ target validation in living *S. aureus* cells with **AV321**. a) Chemical structure of the activity-based photoprobe **AV321**. b) Fluorescence SDS-PAGE analysis of the soluble fraction. c) Volcano plot representation of gel-free quantitative ABPP experiments measured on the Orbitrap XL. Data are derived from three biological replicates for DMSO and **AV321** (5 μM), respectively. The $\log_2$-fold enrichment values were z-score-normalized, and $\log_{10}$(p values) were calculated using a two-sided one-sample Student's t-test. Protein enriched in addition to SaClpP: Protein ID Q2G0P0: 50S ribosomal protein L1. See the Supporting Information for further details and additional analysis.

To explore this finding in more detail, we tested the most potent peptidase inhibitors in a ClpXP protease assay with fluorescent GFP–SsrA (tagged for ClpXP degradation) as a substrate. Indeed, all inhibitors were largely inactive in this assay (Figure S8), demonstrating that ClpX overrides the inhibitor-induced conformational lock. To investigate the mechanistic basis of this unexpected behavior, we utilized a previously introduced activator of ClpP.[14] This compound displaces ClpX in protease assays and was thus used as a surrogate for the chaperone (Figure S9). The molecule abolished **AV286** inhibition of ClpP in casein and peptidase assays in a concentration-dependent manner, which validates a conformational selection of the active enzyme state by ClpX or its surrogates (Figure S9).[15] Our observation is in line with a recent study that showed a conformational switch to the active and extended state upon binding of acyldepsipeptides, which mimic ClpX binding.[5] Thus, regulation by ClpX and other proteolytic activators represents an important and thus far neglected parameter for future ClpP inhibitor development.

In conclusion, **AV145** bound to ClpP arrested the enzyme in an unprecedented inactive conformational state by a significant rotation of Pro125 and an associated misalignment of the catalytic triad architecture. This binding mode was explored for the design of new compounds, which resulted in **AV286**, the first non-covalent inhibitor of ClpP with an

IC$_{50}$ value of < 1 µM. Importantly, ClpX revoked non-covalent binding of the examined inhibitors to ClpP, a counterintuitive finding when compared to related complex proteolytic systems, such as the proteasome, where stable proteolytic inhibitors for individual subunits have been described.[16] Our results therefore strongly imply that regulators such as the ATP-dependent ClpX orchestrate and modulate various distinct conformational stages in the hydrolytic chamber of ClpP. For the identification of non-covalent ClpP inhibitors that are also active in situ, it is thus important not to solely focus on the peptidase activity of the isolated ClpP complex, as this, although easy to monitor, does not accurately reflect the situation in live cells. We hypothesize that sustained ClpP inhibition may either be achieved by increasing the small-molecule-induced conformational lock by, for example, the incorporation of large ligands that block the proteolytic channel, or by inhibitor discovery with the intricate ClpXP proteolytic complex. Both would certainly represent attractive starting points for the future optimization of antivirulence compounds against *S. aureus* and its antibiotic-resistant strains.

Acknowledgements

[1] a) T. A. Baker, R. T. Sauer, *Biochim. Biophys. Acta Mol. Cell Res.* **2012**, *1823*, 15–28; b) J. Ortega, S. K. Singh, T. Ishikawa, M. R. Maurizi, A. C. Steven, *Mol. Cell* **2000**, *6*, 1515–1521; c) J. A. Alexopoulos, A. Guarne, J. Ortega, *J. Struct. Biol.* **2012**, *179*, 202–210.

[2] M. Gersch, A. List, M. Groll, S. A. Sieber, *J. Biol. Chem.* **2012**, *287*, 9484–9494.

[3] F. Ye, J. Zhang, H. Liu, R. Hilgenfeld, R. Zhang, X. Kong, L. Li, J. Lu, X. Zhang, D. Li, H. Jiang, C. G. Yang, C. Luo, *J. Biol. Chem.* **2013**, *288*, 17643–17653.

[4] S. R. Geiger, T. Bottcher, S. A. Sieber, P. Cramer, *Angew. Chem. Int. Ed.* **2011**, *50*, 5749–5752; *Angew. Chem.* **2011**, *123*, 5867–5871.

[5] M. Gersch, K. Famulla, M. Dahmen, C. Gobl, I. Malik, K. Richter, V. S. Korotkov, P. Sass, H. Rubsamen-Schaeff, T. Madl, H. Brotz-Oesterhelt, S. A. Sieber, *Nat. Commun.* **2015**, *6*, 6320.

[6] a) M. W. Hackl, M. Lakemeyer, M. Dahmen, M. Glaser, A. Pahl, K. Lorenz-Baath, T. Menzel, S. Sievers, T. Bottcher, I. Antes, H. Waldmann, S. A. Sieber, *J. Am. Chem. Soc.* **2015**, *137*, 8475–8483; b) T. Böttcher, S. A. Sieber, *Angew. Chem. Int. Ed.* **2008**, *47*, 4600–4603; *Angew. Chem.* **2008**, *120*, 4677–4680.

[7] a) M. Gersch, F. Gut, V. S. Korotkov, J. Lehmann, T. Bottcher, M. Rusch, C. Hedberg, H. Waldmann, G. Klebe, S. A. Sieber, *Angew. Chem. Int. Ed.* **2013**, *52*, 3009–3014; *Angew. Chem.* **2013**, *125*, 3083–3088; b) M. Gersch, R. Kolb, F. Alte, M. Groll, S. A. Sieber, *J. Am. Chem. Soc.* **2014**, *136*, 1360–1366.

[8] F. Weinandy, K. Lorenz-Baath, V. S. Korotkov, T. Bottcher, S. Sethi, T. Chakraborty, S. A. Sieber, *ChemMedChem* **2014**, *9*, 710–713.

[9] A. Cole et al., *Cancer Cell* **2015**, *27*, 864–876.

[10] A. Szyk, M. R. Maurizi, *J. Struct. Biol.* **2006**, *156*, 165–174.

[11] a) M. J. Evans, B. F. Cravatt, *Chem. Rev.* **2006**, *106*, 3279–3301; b) P. P. Geurink, L. M. Prely, G. A. van der Marel, R. Bischoff, H. S. Overkleeft, *Top. Curr. Chem.* **2012**, *308-319*, 85–113.

[12] a) Z. Li, P. Hao, L. Li, C. Y. J. Tan, X. Cheng, G. Y. J. Chen, S. K. Sze, H.-M. Shen, S. Q. Yao, *Angew. Chem. Int. Ed.* **2013**, *52*, 8551–8556; *Angew. Chem.* **2013**, *125*, 8713–8718; b) V. V. Rostovtsev, J. G. Green, V. V. Fokin, K. B. Sharpless, *Angew. Chem. Int. Ed.* **2002**, *41*, 2596–2599; *Angew. Chem.* **2002**, *114*, 2708–2711; c) C. W. Tornøe, C. Christensen, M. Meldal, *J. Org. Chem.* **2002**, *67*, 3057–3064; d) R. Huisgen, *Proc. Chem. Soc.* **1961**, 357–396.

[13] P. J. Boersema, R. Raijmakers, S. Lemeer, S. Mohammed, A. J. Heck, *Nat. Protoc.* **2009**, *4*, 484–494.

[14] D. W. Carney, C. L. Compton, K. R. Schmitz, J. P. Stevens, R. T. Sauer, J. K. Sello, *ChemBioChem* **2014**, *15*, 2216–2220.

[15] M. Merdanovic, T. Mönig, M. Ehrmann, M. Kaiser, *ACS Chem. Biol.* **2013**, *8*, 19–26.

[16] E. M. Huber, M. Groll, *Angew. Chem. Int. Ed.* **2012**, *51*, 8708–8720; *Angew. Chem.* **2012**, *124*, 8838–8850.